Construction of Very Low-Cost Loop Polymerase Chain Reaction System Based on Proportional-Integral-Derivative Temperature Control Optimization Algorithm and Its Application in Gene Detection
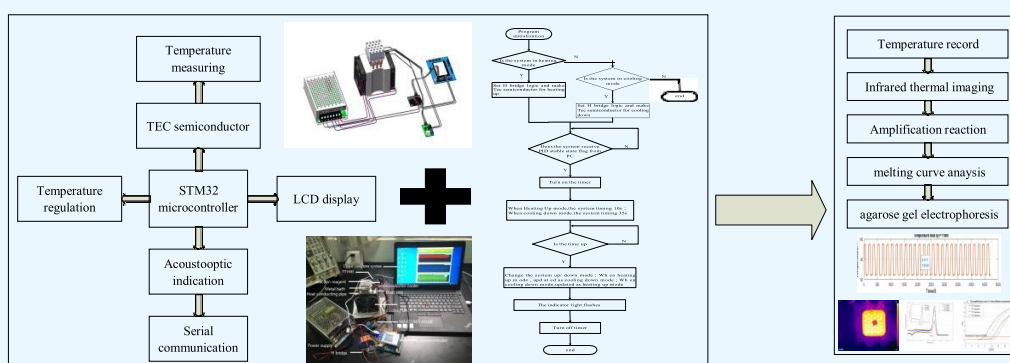
Liping Yao, Yangyang Jiang, Zhongwei Tan, and Wenming Wu*

ACCESS | Metrics & More | Article Recommendations

ABSTRACT: Real-time polymerase chain reaction (PCR) technology is essential in nucleic acid detection and point-of-care testing (POCT). However, nowadays, the classical qPCR instrument has the deficiency of its bulky volume, high cost, and inconvenience to use; hence, a low-cost and easy-to-use PCR equipment was thus developed consisting of a hardware subsystem as well as a software subsystem based on an improved proportional-integral-derivative (PID) system. The proposed system not only could hold self-setting reaction cycles of temperature rising and falling automatically but also the temperature during the constant temperature stage was regulated steady based on improved temperature control algorithm, which proved its great effect compared with the reaction temperature derived from an infrared thermal imaging camera. The experimental results in gene detection research also could indicate its applicability and stability of our developed PCR system by using the amplification curve analysis, the melting curve analysis, and agarose gel electrophoresis analysis compared with the commercial PCR instrument, which illustrates the great potential application value of the proposed PCR system.

1. INTRODUCTION

Polymerase chain reaction (PCR) technology developed in 1983 by Kary Mullis has been a well-known method and has been used widely in biological and medical invention.[1−3] By applying this technology, the natural replication process of DNA and specific DNA molecular fragment amplification in vitro could be obtained, which has been popularized and applied in the detection of various pathogenic microorganisms and parasites,[4] especially in the point-of-care testing (POCT), such as disaster rescue,[5,6] quarantine,[7,8] and plant disease monitoring.[9,10] There exist three stages in a PCR system, namely, denaturation, anneal, and extension.[11,12] When the reagent is heated up to approximately 95 °C, the double-stranded DNA would be dissociated into a single one and combined with the primer in the next round of reactions, which is called as the denaturation of the template DNA stage. While the system's temperature dropped to presumably 55 °C,

the template of the single-strand DNA combined with the primer based on the principle of complementary base pairing, which is called as the annealing of the template DNA and the primer stage. When the dNTP acts as the reaction material and the target sequence as a template under the action of Taq DNA polymerase, in accordance with the principle of complementary base pairing and semiconservative replication, the combination between the template of the single-strand DNA and primer would develop a new semireserved

replication strand complementary to the template DNA strand, which is called the extension of the primer stage. The work accomplishment of cycle denaturation−anneal−extension needs some time,[13] that is, the more semireserved replication strands could be achieved as the new template for the next cycle under the cycle−denaturation−anneal−extension repeat process, and the gene would be amplified several million times in 2−3 h.[14] The PCR technology gives access to a method of amplifying DNA molecules with several orders of magnitude by utilizing the biological and chemical components to orchestrate enzymatic amplification, which has accelerated fundamentally the pace of research in biological and medical fields.[15,16]

The parameter temperature is the fundamental element for the PCR system in biochemical reactions.[17] The optimum target temperature was usually dependent on the reaction situation or the physical characteristics of the molecules in a particular solvent and so forth. The precise control of the sample temperature was critical during the sample reaction and separation process in a PCR system.[18,19] Besides, temperature might affect the reaction rate or efficiency for the system. The over-low system temperature might produce nonspecific priming of templated DNA or form primer-dimers. On the other hand, if the temperature is very high, little or no product will be produced, which thus reduced the PCR yield. Hence, the system temperature optimization plays an important role in a PCR system.[20,21]

In recent years, PCR has been widely used for nucleic acid analysis and biomarker detection. The quantitative-reverse transcriptase PCR (qRT-PCR) reported its improvement in the detection sensitivity of the microRNAs in cancer cells and tissues[22] and showed its high sensitivity in the different microRNAs in lung cancer tissues at the single-molecule level.[23] Li et al. proposed the measurement of trace ricin based on the modified monoclonal antibodies sandwiched sensing mode by using the immuno-gold nanoparticles (IPCR),[24] and the quantitative-reverse transcription PCR (qRT-PCR) was also applied in miRNA detection.[25] With the rapidly development of PCR technology, the PCR machines are thus produced mainly including conventional PCR, gradient PCR, in situ PCR, and quantitative real-time PCR (qPCR).[26−29] As far as the conventional PCR is concerned, the detection of amplified products generally depended on electrophoretic gel analysis, which was time-consuming and hard to quantify the target molecules. Compared with conventional PCR, qPCR contained the entire composition of requirements by including the fluorescence signal acquisition system and the computer analysis processing system.[16] The introduced fluorescein marked the primers and subsequently the primers as well as fluorescent probes combined with the template. The fluorescence signal acquisition system would be in charge of amplification collection, and the computer analysis processing system would obtain the quantitative real-time output results. The qPCR solved the pivotal problems in the conventional PCR; however, the cost was usually approximately 10 times compared to the one of conventional PCR. For example, commercial PCR instruments, such as the Applied Biosystems (ABI) PRISMfi 7900HT, Bio-Rad iQ5 systems, and so forth, have been used extensively with greater detection performance, but their cost is expensive, their volume is bulky, and their operation is complex.[30,31] Based on this fact, we developed a novel PCR system with advantages of low cost, small size, as well as user-friendly software system. The system includes

mainly a hardware control circuit system and a software function system. The hardware control circuit system generally includes a temperature acquisition sensor, a data processing unit, a signal communication unit, a current direction control modular, a microcontrol system, and temperature regulator installation including semiconductor cooler TEC and a pair of cooling electronic fan, which is elaborated in the following. Besides, the control scripts of the microcontroller was prewritten to implement the control effect of the system, LCD information display, status indication, and communication function. The computer software was also designed for the simple system setup, intuitive process display, and subsequent data analysis. Besides, the experiment in gene detection based on the commercial qPCR instrument and our proposed system is also performed and analyzed in this study. The rest of this study is organized as follows: in Section 2, the used reaction reagents and the proposed PCR system by including a hardware subsystem and a software subsystem is explained. In Section 3, the experimental results are presented. Finally, the article is concluded in Section 4.

2. MATERIALS AND METHODS

2.1. Reagents. The performance of the proposed PCR system was verified compared with that of the commercial qPCR instrument (ABI 7500, USA) to detect the DNA segments of SEC61 translocon subunit alpha, Matrix Metallopeptidase, and ORF1ab. The PCR primers of each DNA segment were designed by Primer Express 3.0. The sequence of the forward primer and the reverse primer from ranslocon subunit alpha, Matrix Metallopeptidase, and ORF1ab are listed in the following Table 1.

Table 1. Primer Sequences of Genes

genes	primer sequences
template 1: SEC61 translocon subunit alpha	F:5′-AGATGGGTGCTGGAATCTGC-3′R:5′-CAAATTCCATCCCTCGGCCA-3′
template 2: matrix metallopeptidase	F:5′-GCCCCCATGAAGCCTTGTTT-3′R:5′-GCTGGTGCAGCTCTCATACT-3′
template 3: ORF1ab	F:5′CCCTGTGGGTTTTACACTTAA-3′R:5′ACGATTGTGCATCAGCTGA-3′

2.2. PCR Hardware Subsystem. The designed PCR system included the hardware and software subsystems. As could be seen in Figure 1, the lower computer hardware part of the designed PCR system mainly contained a reagent placement unit, a temperature detection unit, a temperature control unit, a status indication unit, a communication unit, a power supply unit, and so forth. They were connected with
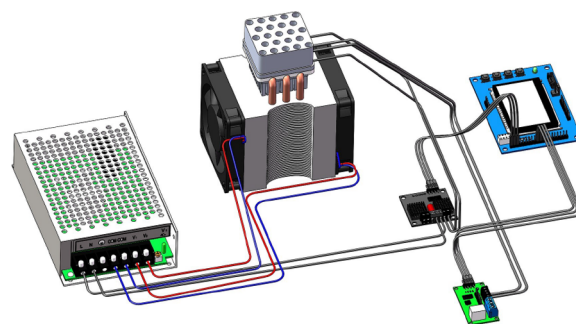
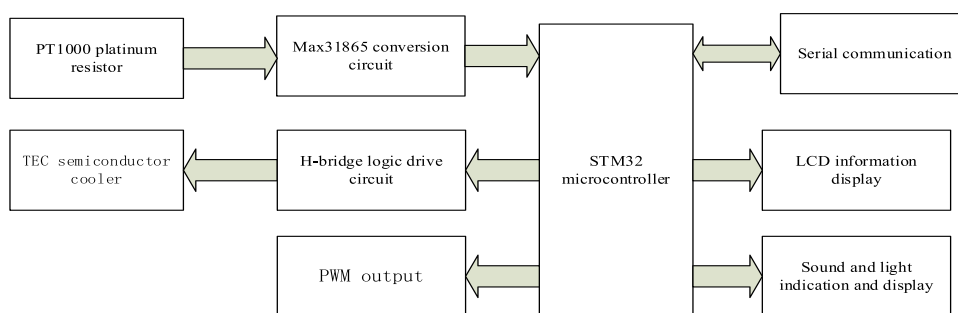**Figure 1.** Composition of the hardware system.

Figure 2. Structure diagram of the designed PCR system.

each other orderly and logically to realize the comprehensive system function. The STM32 microcontroller was used as the control core of the system. The platinum resistance PT1000 and MAX31865 circuits were used for temperature acquisition and conversion, respectively.[32] The chosen PT1000 holds the advantage of small volume, high measurement accuracy, and good stability, and the MAX31865 contains the 15-bit high-resolution Σ-Δ ADC to obtain more accurate temperature information. The microprocessor showed the real-time digital temperature through SPI communication with max31865. The model ATE1-TC-127-8AH was chosen as the refrigeration and heating elements of the system, which was on the basis of the principle that the P-N junction was made of semiconductor materials to form thermocouple pairs and then produced the Peltier effect. The thermoelectric cooler could be set as cooling or heating by changing the current direction flowing through TEC. Thus, the H bridge logic control drive circuit, which satisfied the power level of the system, was selected to regulate the current direction so that the cooler TEC could be set as temperature rise or fall mode of the system. Meanwhile, the pulse width modulation technology was implemented in power regulation of the cooler TEC. That is, the high and low levels at different times was generated through PWM duty cycle setting to control the working time of the semiconductor cooler, and the refrigeration efficiency was thus regulated. Besides, the heat conducting pipe, heat sink, and a pair of electric ventilating fans were designed for heat conduction of the system. The LCD of the microcontroller would display the system information, such as real-time temperature, the regulated power, and the state information. Meanwhile, the indicator light would accompany the system running, and the alarm would take effect while the system runs under abnormal circumstances. The structure diagram of the designed PCR system is shown in Figure 2.

2.3. PCR Software Subsystem. The software design in the PCR system included mainly the embedded software part and the computer programming part. In the embedded microcontrol system, the system information would be displayed through LCD, and the temperature was collected in real time by PT1000 and MAX31865 modular. The microprocessor used the SPI communication method to obtain the digital temperature, which was transformed into digital signals, and subsequently, it was transfer to the computer. As could be seen in Figure 3a, the system would be in heating mode in the outset when the system parameters are set and ready for operation, and the system would update its temperature change mode based on the PID temperature regulation algorithm and the set reaction time. Specifically, after the system received the stable state signal from the PID control method, the system was in heating mode, the duration

of which lasted for 10 s based on the timer, while the duration was 30 s when it was in the cooling mode. After the system timing is completed, it would change the reaction mode by setting up the H bridge logic unit. Besides, the embedded microcomputer system received the power value calculated from improved PID algorithm and applied this power value as the PWM duty cycle to regulate the heat efficiency of the TEC, in order to regulate temperature to the appropriate location.

The computer programming was responsible mainly for serial communication modular, graphic curve display such as the temperature curve, PID control power curve, temperature gradient curve, signal data preservation, and subsequent data processing methods except the improved PID temperature control algorithm. The improved PID algorithm would be introduced as follows.

The conventional PID algorithm was composed of the proportion element, integration element, and differentiation element, which was a classical control method in engineering.[33] The block diagram of the PID control algorithm is indicated in Figure 3b, and the equation is shown as follows:

$$u(t) = K_P\left[e(t) + \frac{1}{T_I}\int e(t)\mathrm{d}t + T_D\frac{\mathrm{d}e(t)}{\mathrm{d}t}\right] \tag{1}$$

Here, $e(t)$ is the temperature error value, $u(t)$ is the PID output value, and K_P, T_I, T_D are the proportion coefficient, integration coefficient, and differentiation coefficient, respectively.

Thus, it could be seen that the system power would be amended through computing the proportion one, integration one, and differentiation one on the basis of the temperature error value. However, the experimental results found that the system might exhibit an overshoot phenomenon by using the conventional PID algorithm. Based on this, the optimized PID algorithm by amending the parameter, introducing filtering method, and optimizing the integral component was implemented and applied on our PCR system in this study, which could prove its great performance to overcome the overshoot phenomenon of the system, as could be seen in Figure 4. The improved PID algorithm would be elaborated in the following.

2.3.1. Optimized PID Algorithm. **Input:** Actual temperature value, given the target temperature value.

Output: The power value for PWM

(1) Initial the parameter, including K_P, K_I, and K_D;

(2) Amend the parameter on the basis of the actual temperature;

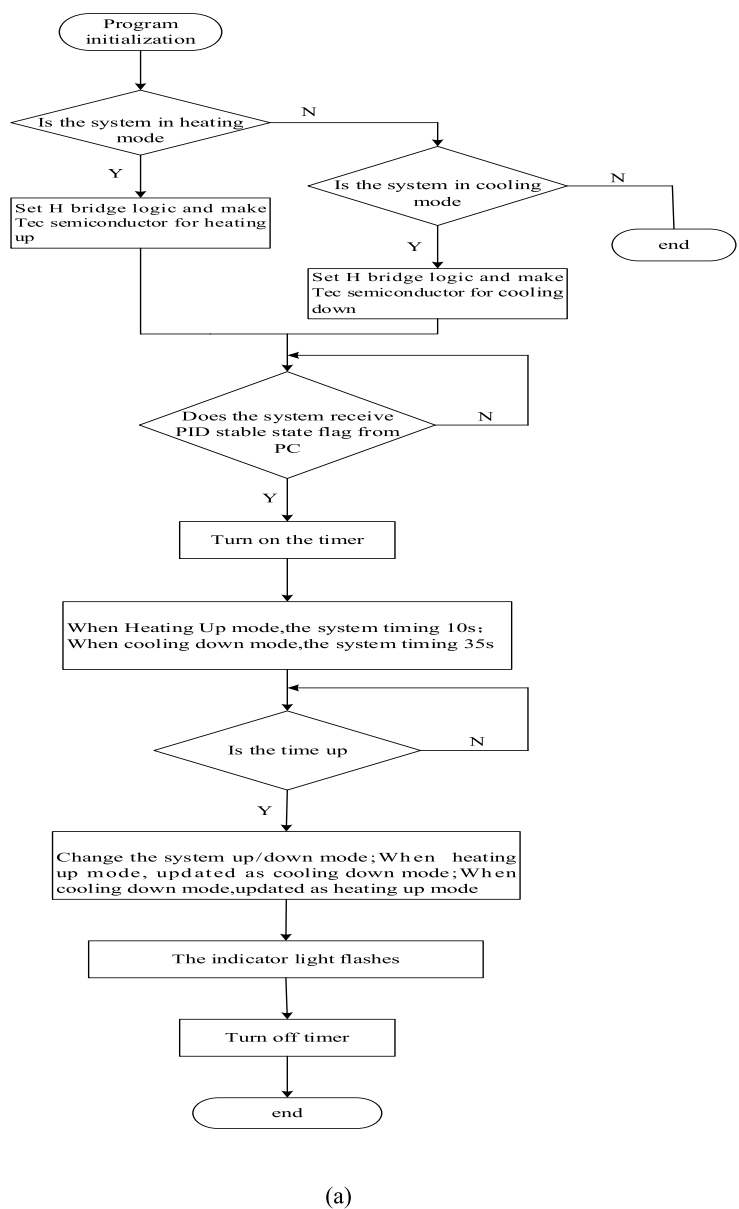The filter method is introduced in the oscillatory interference removal; calculate temperature difference between

(a)

(b)

Figure 3. (a) Temperature rise and fall mode regulation of the system. (b) Basic principle block diagram of the PID control algorithm.

the current actual temperature value and the given target temperature value.

(3) The calculation of the PID values

Calculate the Pout in the light of the temperature difference value and the parameter K_P. Here, the *threshold_1* and *threshold_2* are two-thirds and one-third of the *threshold_4*. The *threshold_4* is the overall PID output value of the system.

The *threshold_3* is the zero point one of the gap between the designed lower temperature and higher temperature.

If current PID output > *threshold_1*, accumulate the negative difference value;

If current PID output < *threshold_2*, accumulate the positive difference value;

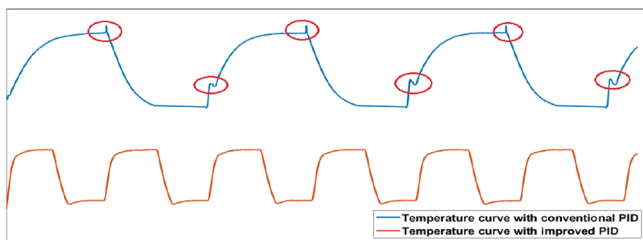If the difference value > *threshold_3*, no integral operation;

Figure 4. Results of the conventional PID algorithm and the optimized PID algorithm.

If the difference value < *threshold_3*, perform variable speed integration function, as shown in eq 2.

$$f(e(k)) = \begin{cases} 1 & |e(k)| \leq f \\ \dfrac{f + g - |e(k)|}{f} & f \leq |e(k)| \leq f + g \\ 0 & |e(k)| > f + g \end{cases} \qquad (2)$$

Here, $[f, f + g]$ is the variable speed range, and the variable speed coefficient $f(e(k))$ is a function of variable $e(k)$.

Calculate the Dout in the light of the difference and parameter K_D;

Thus, the PID value $u(k)$ would be computed, as shown in eq 3.

$$u(k) = K_P e(k) + f(e(k)) K_I \sum_{j=0}^{k} e(j) + K_D[e(k) - e(k-1)] \qquad (3)$$

Then, limit the range of the PID output value $u(k)$, that is:
If $u(k) > +threshold\_4$:
$u(k) = +threshold\_4$;
If $u(k) < -threshold\_4$:
$u(k) = -threshold\_4$;

(4) Output:

The current temperature regulation mode of the system is determined, and the PID output value is sent out as the PWM

Table 2. Cost Estimation of the Proposed System

Device	Equipment cost(¥)	Service cost(¥)	Labour cost(¥)	Equipment volume	Operating software
The proposed system	781	--	--	--	--
The portable power	169				
Temperature probe + acquisition modular	75				
H bridge current control circuit	67	36000	48000	Small	Easy to use and friendly interface
Micro controller + LCD display	122				
Metal orifice plate-TEC+heat pipe+ heat sink+ ventilating fans	348				
The commercial qPCR instrument (ABI 7500, USA)		285000		Large	friendly interface,but Complex operation

(a)

(b)

Figure 5. Experimental PCR system and device. (a) Designed PCR system and (b) commercial qPCR instrument.

(a)

(b)

(c)

(d)
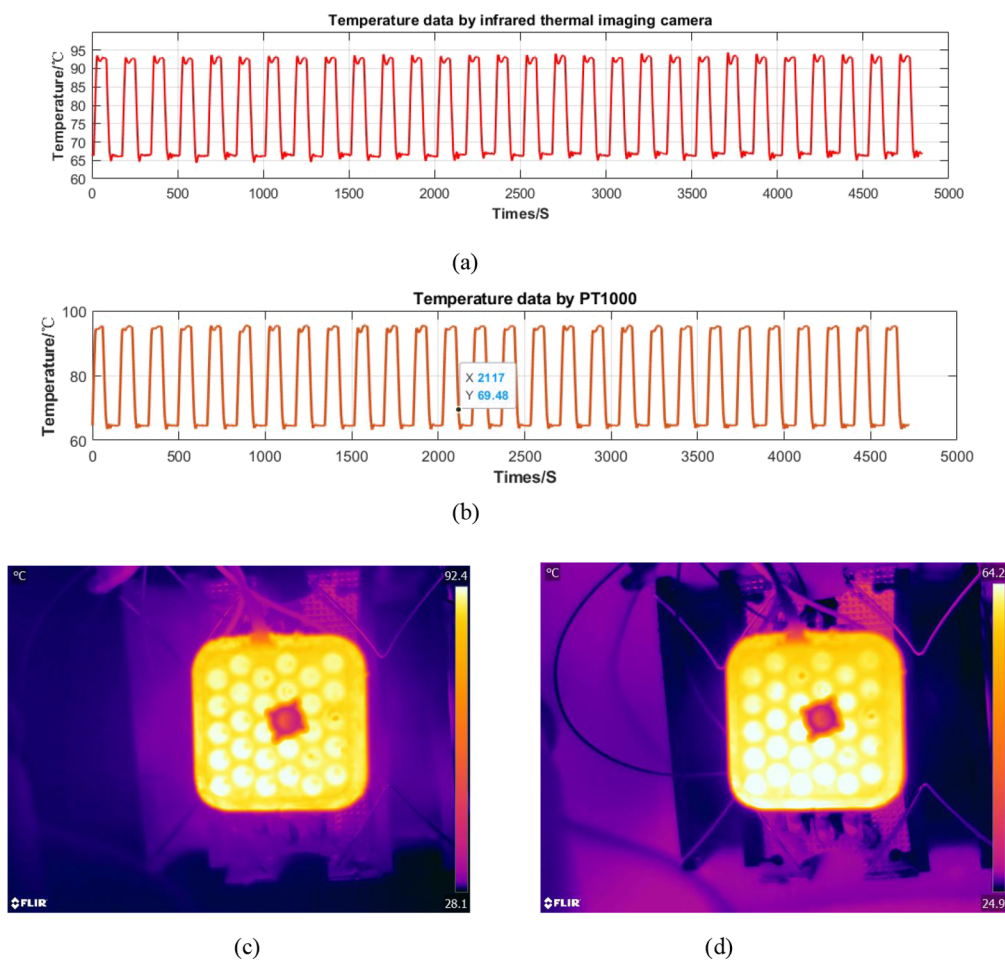
Figure 6. (a) Temperature curve from the infrared thermal imaging camera. (b) Temperature curve from the PT1000 platinum thermistor. (c) Infrared thermal imaging of higher heating up temperature. (d) Infrared thermal imaging of lower cooling temperature.

duty cycle in this temperature regulation mode to the microcontroller by using the serial communication.

It is judged whether the temperature could be regulated greatly and steadily on the basis of the parameter $err_{max}(k)$.

If $err_{max}(k) <$ threshold_5

    Send(stable_flag = 1)

2.4. Cost Estimation of the System. We have made the system cost estimation comprehensively so as to explain the greater performance of the proposed system. As indicated in Table 2, we consider the cost of each component belonging to this system, and the overall equipment cost just reached ¥781. Besides, we also consider the service cost and labor input of this system. The estimation of the service cost needs nearly 3.6 million yuan, and the consumption of the labor input needs 4.8 million yuan for system development and system maintenance. Therefore, the total cost of the proposed system would reach nearly 8.5 million yuan. Under the circumstance that the
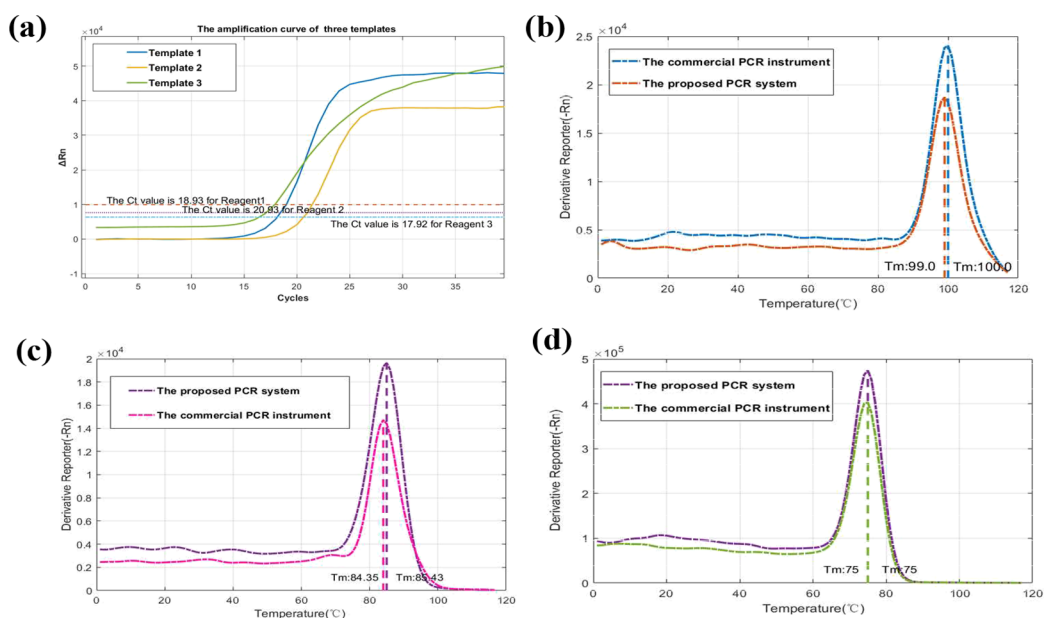
Figure 7. Amplification curves and melting curves of three different reaction templates (a−d).
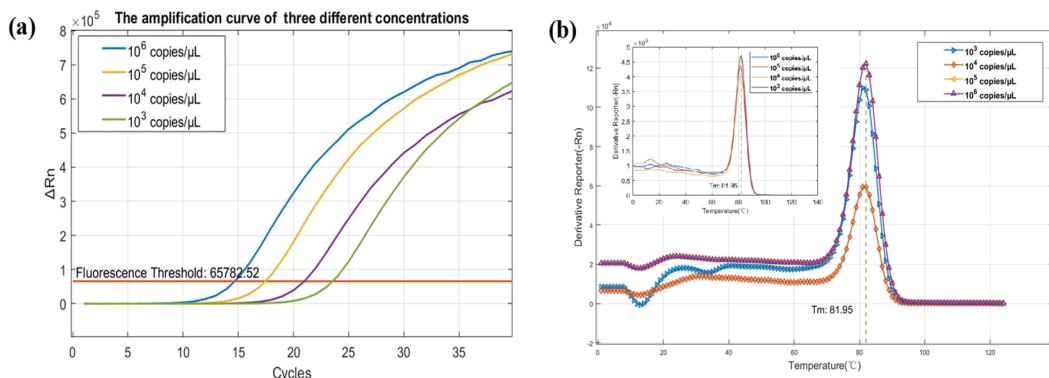

Figure 8. Amplification curves and melting curves of the reagents with four different gradient concentrations (a−b).

proposed product could achieve similar effects with commercial equipment ABI 7500, our designed system holds the advantage of very low cost, smaller volume, and being user, which could show its huge application potential.

3. RESULTS AND DISCUSSION

3.1. Experimental PCR System and Device. The designed PCR system is displayed in Figure 5a, which was composed of the hardware subsystem and the PC software subsystem. The reaction reagent was placed on the metal bath, and the temperature would be changed from 65 to 95 °C circularly by the system. Every system module was also marked out clearly. Meanwhile, the commercial qPCR instrument (ABI 7500, USA) was also used in the PCR reaction so as to analyze and compare with our system in this study, as shown in Figure 5b.

3.2. Temperature Control Analysis. The PCR system could monitor the system's temperature because the temperature sensor was embedded in an aluminum plate. The temperature variation during the PCR reaction is a pivotal factor to estimate the performance of the reaction.[34] Thus, the original real-time system temperature collected by platinum resistance was recorded. To assess the accuracy of the measured temperature, the infrared thermal imaging camera

(FLIR T620, USA) was also used to collect data stream, which could be exported to further inspect the uniformity of the temperature. The two temperature change curves are shown in Figure 6a,b. We could see that the temperature was increased up to 95 °C and cooled to 65 °C and concurrently being last for the specific time steadily. On the other hand, because the temperature sensor was embedded in the aluminum plate and the reagent was placed on the metal bath, the temperature of the infrared thermal imaging camera was slightly lower compared to that collected by PT1000. Besides, Figure 6c,d displays the higher heating temperature and lower cooling temperature of the infrared images, respectively. Generally, these two temperature variation curves are consistent and further illustrate good thermal uniformity of the aluminum plate for this system, benefiting from the improved PID temperature control algorithm.

3.3. Analysis of the Reagents with Different Templates. The reagent is amplified 40 cycles during the reaction by introducing the three different templates, as indicated in Table 1, by using the PCR system and commercial qPCR instrument ABI 7500. Figure 7 displays the amplification and melting curves of three different reaction templates, as indicated in Table 1. The number of cycles for the intersection from the fluorescence threshold and the

amplification curve is the C_t value. The fluorescence thresholds of Templates 1, 2, and 3 are chosen as 9960, 7627, and 6354, respectively, and thus, the C_t values of the corresponding reagents are 18.93, 20.93, and 17.92, separately, which are displayed clearly in the amplification curve in Figure 7a and indicate that the reagent performed the biological reaction over 10 cycles, and it would achieve the fastest reaction rate at almost 20 cycles and reach the maximal reaction value during the process at approximately 25 cycles. Besides, we also analyzed the melting curves of the designed PCR system and commercial PCR instrument. As we know, the temperatures of the different DNA double helix structures were distinct when the melting rate arrived at the fastest speed; hence, there would be different characteristic peaks (T_m). Therefore, the value Tm could be used to determine the only product from the DNA amplification. As could be seen in Figure 7b−d, the characteristic peak all appeared at the same temperature from the proposed PCR system and commercial PCR instrument. Moreover,

the different template holds the distinct characteristic peaks Tm, which could demonstrate that the product was relatively pure, and the system could distinguish simultaneously different templates.

3.4. Analysis of the Reagents with Different Gradient Concentrations. The reagents with four different gradient concentrations at 106, 105, 104, and 103 copies/μL were also used to examine the amplification reaction, as shown in Figure 8a. The fluorescence threshold of the reagent was set as 65,782.52, the C_t value of the reagents at the four different concentrations were 14.70, 17.46, 20.96, and 23.56 cycles, respectively. In addition, the reagents at the higher concentration would react before the one at lower concentration, which could distinguish four reagents at different concentrations evidently. Figure 8b shows the melting curves of the templates with four different gradient concentrations at 10^6, 10^5, 10^4, and 103 copies/μL from both the proposed PCR system and commercial PCR instrument. As we could see, the characteristic peak all appeared at the same temperature, which could demonstrate that the product was relatively pure, and we further check the specificity of the PCR assay.

Besides, the templates with four different gradient concentrations gained from the designed PCR system and the commercial PCR instrument were further tested by agarose gel electrophoresis after reaction. As represented in Figure 9, the first four lanes in the left represented the target amplicon of the reagents at four different gradient concentrations by using the proposed PCR system, and the other four lanes in the right showed the results of the reagents from the commercial PCR

Figure 9. Testing results of the agarose gel electrophoresis.

instrument. The agarose gel electrophoresis testing image demonstrated that the DNA amplification results obtained by using the proposed PCR system and commercial PCR instrument were similar, and the one single peak in the melt curve in Figure 8b corresponded to a single band on the gel image, which also demonstrated that the reaction product was relatively pure without other primer-dimers.

4. CONCLUSIONS

PCR technology has been developed rapidly, and therefore, PCR devices are exploited a lot in succession. Based on the fact that there exists the disadvantages of high cost, bulky volume, and complex operation for users with regard to the current commercial PCR instruments, in this study, a novel PCR system was proposed and analyzed in gene detection. The system consists of a hardware subsystem and a software subsystem. The hardware subsystem could mainly support the temperature detection, collection, and control. Moreover, it also supports information transmission, process LCD display, and status indication. The software subsystem could implement the coordination control and stable operation of the system. Besides, the improved PID temperature control algorithm was proposed to solve the overshoot phenomenon, and the great temperature regulation effort would be further proved by using the infrared thermal imaging camera and the PT1000 platinum thermistor. On the other hand, the experiments performed on our PCR system and commercial PCR instrument ABI 7500 with different templates and different concentrations were also used to analyze the reliability and performance of our system. The experimental results indicated that the system could exhibit normal responses of the reagents and distinguish different templates for the reaction under three different templates, and the different concentrations could also be distinguished evidently because the amplification curves with the templates at four different gradient concentrations at 106, 105, 104, and 103 copies/μL were 14.70, 17.46, 20.96, and 23.56 cycles, respectively. The melting curve and agarose gel electrophoresis analysis further demonstrated that the product was relatively pure without other primer-dimers because of the single characteristic peaks (T_m) and nonspecific bands. Besides, we also made the cost estimation of our system. The total cost of the proposed system would be reached at nearly 8.5 million yuan, which is far less than that of other commercial PCR instruments, and the equipment ABI 7500 needs up to 28.5 million yuan. Besides, based on the conclusion that our proposed system could achieve basically the same detection effect with the commercial PCR instruments, our proposed system could also embody its advantage of the smaller volume and user-friendly software system, which holds a great application prospect in biological and medical fields.

■ AUTHOR INFORMATION

Corresponding Author

Wenming Wu − *Institute of Biological and Medical Engineering, Guangdong Academy of Sciences, Guangzhou 510500, China; State Key Laboratory of Microelectronics and Integrated Circuits, Fudan University, Shanghai 200433, China;* ⊙ orcid.org/0000-0003-4793-6132; Email: wuwenming627@163.com

Authors

Liping Yao − *Institute of Biological and Medical Engineering, Guangdong Academy of Sciences, Guangzhou 510500, China*

Yangyang Jiang − *Institute of Biological and Medical Engineering, Guangdong Academy of Sciences, Guangzhou 510500, China*

Zhongwei Tan − *Institute of Biological and Medical Engineering, Guangdong Academy of Sciences, Guangzhou 510500, China*

Complete contact information is available at:
https://pubs.acs.org/10.1021/acsomega.2c02975

Notes

The authors declare no competing financial interest.

■ REFERENCES

(1) Mullis, K. B. The polymerase chain reaction (Nobel Lecture). *Angew. Chem., Int. Ed. Engl.* **1994**, *33*, 1209−1213.

(2) Rakhmatulina, M. R.; Galkina, I. S. Quantitative PCR in diagnosing infectious urogenital pathology. *Sex. Transm. Infect.* **2019**, *2021*, 107−111.

(3) Yates, T. A.; Cooke, G. S.; MacPherson, P. Rational use of SARS-CoV-2 polymerase chain reaction tests within institutions caring for the vulnerable. *F1000Res.* **2020**, *9*, 671.

(4) Wang, H.; Zhang, C.; Xing, D. Simultaneous detection of Salmonella enterica, Escherichia coli O157: H7, and Listeria monocytogenes using oscillatory-flow multiplex PCR. *Microchim. Acta* **2011**, *173*, 503−512.

(5) Tran, N. K.; Godwin, Z.; Bockhold, J.; Kost, G. J. Point-of-care testing at the disaster-emergency-critical care interface. *Point Care* **2012**, *11*, 180.

(6) Mecozzi, D. M.; Brock, T. K.; Tran, N. K.; Hale, K. N.; Kost, G. J. Evidence-based point-of-care device design for emergency and disaster care. *Point Care* **2010**, *9*, 65−69.

(7) Li, Y., Zhang, H., Zhang, P.*Application of UPT-POCT in Import and Export Quarantine[M]//Principles and Applications of Up-converting Phosphor Technology*; Springer: Singapore, 2019: 191−199.

(8) Wu, D.; Shi, B.; Li, B.; Wu, W. A Pipeline-Based Oil-Bath PCR Method for Bacteria Detection. *IEEE Access* **2020**, *8*, 99598−99604.

(9) Subekti, D.; Hidayat, S. H.; Damayanti, T. A. Quantitative polymerase chain reaction (Q-PCR) for detection of sugarcane streak mosaic virus. *IOP Conf. Ser: Earth Environ. Sci.* **2020**, *418*, No. 012062.

(10) Sanchez, L.; Pant, S.; Mandadi, K.; Kurouski, D. Raman spectroscopy vs quantitative polymerase chain reaction in early stage Huanglongbing diagnostics. *Sci. Rep.* **2020**, *10*, 10101.

(11) Garibyan, L.; Avashia, N. Polymerase chain reaction. *J. Invest. Dermatol.* **2013**, *133*, 1−4.

(12) Jiang, Y.; Li, B.; Wu, W. Application of automatic feedback photographing by portable smartphone in PCR. *Sens. Actuators, B: Chem.* **2019**, *298*, No. 126782.

(13) van Pelt-Verkuil, E., van Belkum, A., Hays, J. P.*The PCR in practice. Principles and Technical Aspects of PCR Amplification*; Springer Netherlands, 2008: 17−23.

(14) Valasek, M. A.; Repa, J. J. The power of real-time PCR. *Adv. Physiol. Educ.* **2005**, *29*, 151−159.

(15) Lee, S. H. Testing for SARS-CoV-2 in cellular components by routine nested RT-PCR followed by DNA sequencing. *Int. J. Geriatr. Rehabil.* **2020**, *2*, 69−96.

(16) Li, X.; Wu, W.; Manz, A. Thermal gradient for fluorometric optimization of droplet PCR in virtual reaction chambers. *Microchim. Acta* **2017**, *184*, 3433−3439.

(17) Nasser, G. A.; Abdel-Mawgood, A. L.; Abouelsoud, A. A.; Mohamed, H.; Umezu, S.; El-Bab, A. M. New cost effective design of PCR heating cycler system using Peltier plate without the conventional heating block. *J. Mech. Sci. Technol.* **2021**, 3259−3268.

(18) Khaliq, A.; Kafafy, R.; Salleh, H. M.; Faris, W. F. Enhancing the efficiency of polymerase chain reaction using graphene nanoflakes. *Nanotechnology* **2012**, *23*, No. 455106.

(19) Karami, A.; Hasani, M.; Jalilian, F. A.; Ezati, R. Conventional PCR assisted single-component assembly of spherical nucleic acids for simple colorimetric detection of SARS-CoV-2. *Sens. Actuators, B: Chem.* **2021**, *328*, No. 128971.

(20) Kean, O. W. Using the gradient technology of the Mastercycler pro to generate a single universal PCR protocol for multiple primer sets. *Eppendorf, Malasya* **2010**, *220*, 2010.

(21) Kim, H.; Park, N.; Hahn, J. H. Parallel-processing continuous-flow device for optimization-free polymerase chain reaction. *Anal. Bioanal. Chem.* **2016**, *408*, 6751−6758.

(22) Wang, Z. Y.; Li, D. L.; Tian, X.; Zhang, C. Y. A copper-free and enzyme-free click chemistry-mediated single quantum dot nanosensor for accurate detection of microRNAs in cancer cells and tissues. *Chem. Sci.* **2021**, *12*, 10426−10435.

(23) Li, C. C.; Chen, H. Y.; Luo, X.; Hu, J.; Zhang, C. Y. Multicolor fluorescence encoding of different microRNAs in lung cancer tissues at the single-molecule level. *Chem. Sci.* **2021**, *12*, 12407−12418.

(24) JJiang, S.; Liu, Q.; Liu, W. J.; Cui, L.; Zhang, C. Y. Label-free detection of LncRNA in cancer cells with human telomere G-quadruplex DNA-thioflavin T binding-induced fluorescence. *Sens. Actuators, B: Chem.* **2022**, *358*, No. 131521.

(25) Li, Y.; Liang, L.; Zhang, C. Isothermally sensitive detection of serum circulating miRNAs for lung cancer diagnosis. *Anal. Chem.* **2013**, *85*, 11174−11179.

(26) Cullen, D. W.; Lees, A. K.; Toth, I. K.; Duncan, J. M. Conventional PCR and real-time quantitative PCR detection of Helminthosporium solani in soil and on potato tubers. *Eur. J. Plant Pathol.* **2001**, *107*, 387−398.

(27) Zhang, C.; Xing, D. Microfluidic gradient PCR (MG-PCR): a new method for microfluidic DNA amplification. *Biomed. Microdevices* **2010**, *12*, 1−12.

(28) Hussein, E. A.; Mohd, H. B.; Liew, P. S.; Omar, A. R.; Arshad, S. S.; Ideris, A. In situ PCR for detection and differentiation of infectious bursal disease virus strains in chickens. *Online J. Vet. Res.* **2017**, *21*, 644−656.

(29) Pfaffl, M. W. Quantification strategies in real-time polymerase chain reaction. *Quantitative Real-Time PCR Appl. Microbiol.* **2012**, 53−62.

(30) Bialek, H.; Dawes, J.; Heer, D.; Johnston, M. L.Portable real-time PCR system using tablet-based fluorescence imaging[C]// *2016IEEE EMBS International Student Conference (ISC)*; IEEE, 2016, 1−4.

(31) He, L.; Sang, B.; Wu, W. Battery-powered portable rotary real-time fluorescent qPCR with low energy consumption, low cost, and high throughput. *Biosensors* **2020**, *10*, 49.

(32) Li, Y.; Zhan, J.; Xu, W.; Qi, C.; Zhu, C.Design and analysis of high-power thermostatic control system based on TEC*Sixth Symposium on Novel Optoelectronic Detection Technology and Applications*; International Society for Optics and Photonics2020, *11455*, 1145567.

(33) Chen, Y., Xia, F. Y., Xu, B. X.Study of PID control algorithm and intelligent PID controller[C]//Mechatronics and Automation Engineering: *Proceedings of the International Conference on Mechatronics and Automation Engineering (ICMAE2016)*. 2017: 35−43.

(34) Mahanty, A.; Purohit, G. K.; Mohanty, S.; Nayak, N. R.; Mohanty, B. P. Suitable reference gene for quantitative real-time PCR analysis of gene expression in gonadal tissues of minnow Puntius sophore under high-temperature stress. *BMC Genomics* **2017**, *18*, 617.